Electronic Supplementary Information for

Reduced graphene oxide doped predominantly with CF_2 groups as a superior anode material for long-life lithium-ion batteries

Haoran An[1], *Yu Li*[1,3,4], *Yiyu Feng*[1,3,4], *Yu Cao*[1], *Chen Cao*[1], *Peng Long*[1], *Shuangwen Li*[1] *and Wei Feng*[1,2,3,4*]

1. School of Materials Science and Engineering, Tianjin University, Tianjin 300072, P. R China.

2. Collaborative Innovation Center of Chemical Science and Engineering, Tianjin 300072, P. R China.

3. Key Laboratory of Advanced Ceramics and Machining Technology, Ministry of Education, Tianjin 300072, P. R China.

4. Tianjin Key Laboratory of Composite and Functional Materials, Tianjin 300072, P. R China.

Experimental section:

Synthesis of F-rGO. Reduced graphene oxide (rGO) was purchased from Chengdu Organic Chemicals Co. Ltd. Chemical reagents purchased from Tianjin Jiangtian Chemical Company. The reduced graphene oxide was dispersed in a mixture solution

of 25 mL ethanol and 5 mL HF (40 wt%) by stirring for 5 min. Then the dispersion was transferred to a Teflon-lined autoclave followed by heating at 150 °C for 24 h. After cooling to room temperature, the obtained fluorine doped reduced graphene oxide (F-rGO) was washed with deionized water and ethanol to remove residual reagent and dried in a vacuum oven at 60°C for 24 h. For comparison, solvothermal treated reduced graphene oxide (Sol-rGO) were also prepared through the conventional hydrothermal process at 150 °C without adding HF into the dispersion. Graphene oxide (GO) was synthesized from natural graphite using the modified Hummers method. F-doped graphene oxide (F-GO) was synthesized by heating the mixture of GO solution (25 mL 1.0 mg/mL) and hydrofluoric acid (5 mL 40 wt%) at 150 °C for 24 h in a Teflon-lined autoclave. After removing the residual acid, the F-GO was dried through freeze drying.

Characterization. The morphology and surface microstructures were investigated by field-emission transmission electron microscopy (FETEM, JEOL JEM-2100F) and field-emission scanning electron microscopy (FESEM, Hitachi S-4800). Crystal structure was determined by X-ray diffraction (XRD, Rigaku D/max-2500 with Cu Kα radiation). Fourier Transform Infrared (FT-IR) spectra were recorded on a Bruker Tensor 27 spectrometer. Raman scattering was performed on a Raman spectrometer (DXR Microscope, Thermo Electron) using laser excitation at 532 nm. X-ray photoelectron spectroscopy (XPS) analysis was obtained using PERKIN ELMZR PHI 3056 with an Al anode source operated at 15 kV to analyze the chemical composition of the materials. The N_2 adsorption-desorption isotherms were investigated with pore

size analyzer (Autosorb-iQ2-MP, America) and specific surface area was obtained by Brunauer Emmett Teller (BET) methods.

Electrochemical measurements. Electrochemical performances were evaluated by using CR2032 coin cells. To produce working electrodes, F-rGO, F-GO and Sol-rGO was mixed with Super-P carbon black and poly(vinylidene fluoride) with a weight ratio of 80:10:10 in N-methyl-2-pyrrolidone. The mixture slurries were coated on a copper foil. The coating was dried in an oven at 80 ^{o}C overnight. The resulting electrode film was cut into small disks (0.8 cm) with 1-2 mg active materials for the test in coin cells. The coin cells were assembled in a dry argon-filled glove box (Mikrouna Co., Advanced 2440/750), using lithium foil as the counter electrode, the electrolyte was 1.0 M $LiPF_6$ in a 1:1 volume ratio mixture of ethylene carbonate (EC)/dimethyl carbonate (DEC). The discharge/charge performances of assembled LIBs were tested in potential range of 0.01-3.0 V (*vs.* Li^+/Li) at constant current densities (Land CT2001A, Wu Han Jin Nuo Electronics Co., China). Cyclic voltammetry (CV) tests were performed on a CHI660D electrochemical workstation in the same potential range at a scan rate of 0.5 mV s^{-1}. Electrochemical impedance spectroscopy (EIS) was performed from 0.01 to 1 MHz frequency range using VERSASTAT3-100 .

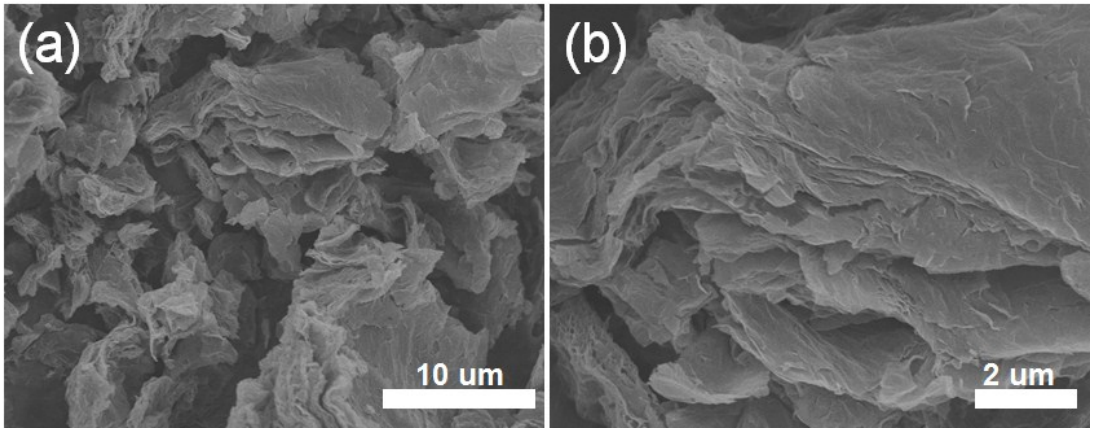

Fig. S1 a) SEM image of Sol-rGO. b) Magnified SEM image of Sol-rGO.

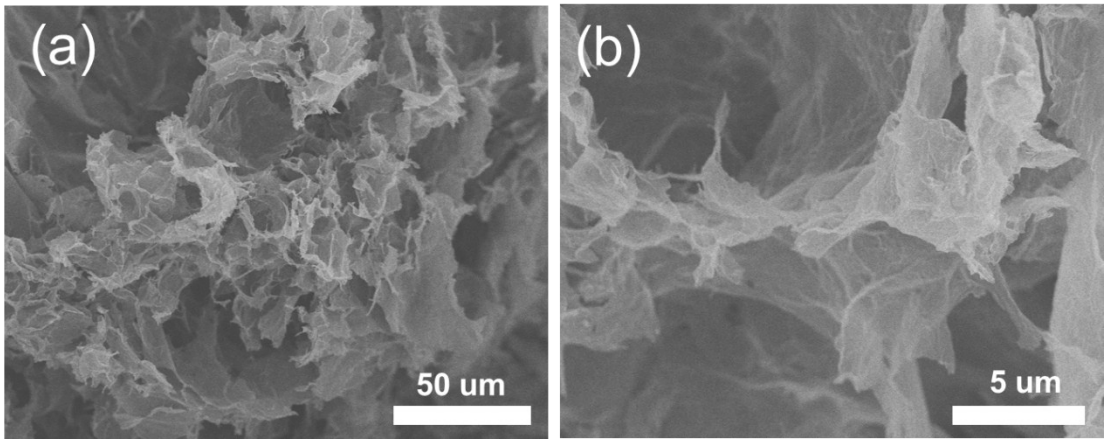

Fig. S2 a) SEM image of F-GO. b) Magnified SEM image of F-GO.

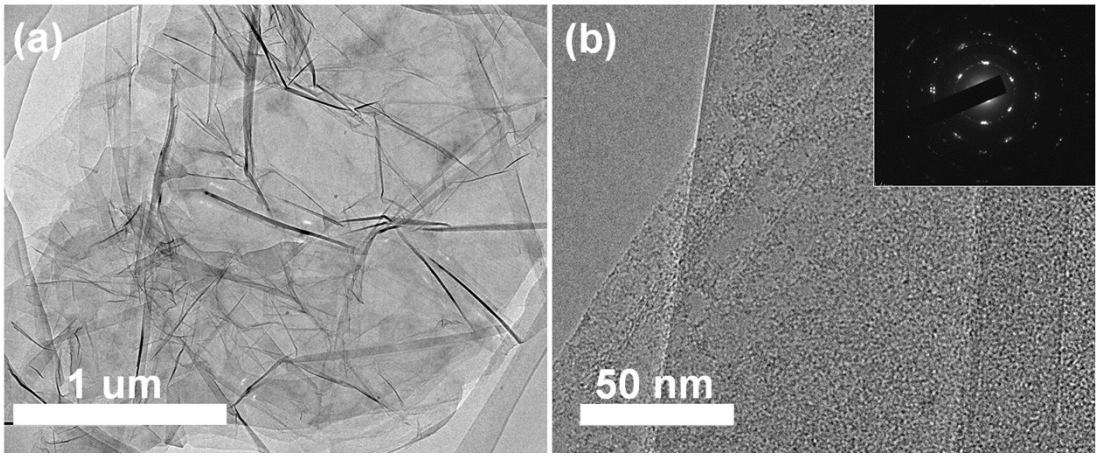

Fig. S3 a) TEM image of Sol-rGO. b) HR-TEM image of Sol-rGO (inset shows the corresponding SEAD).

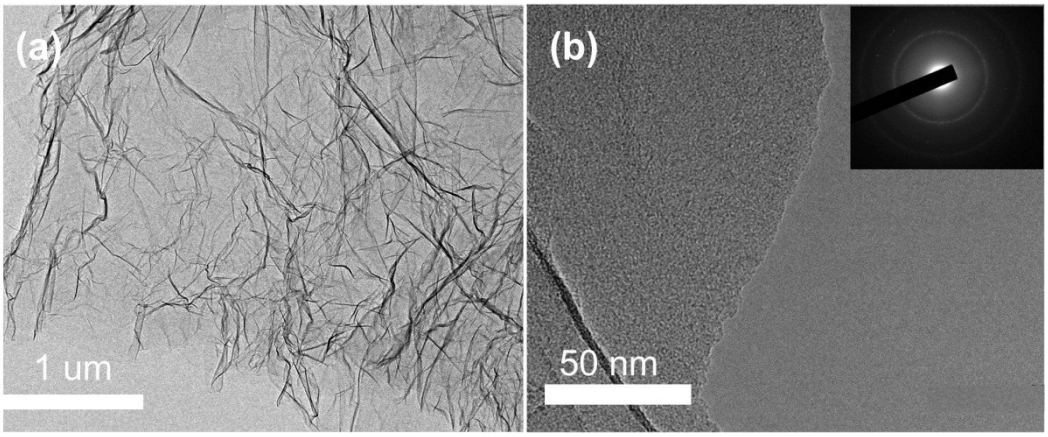

Fig. S4 a) TEM image of F-GO. b) HR-TEM image of F-GO (inset shows the corresponding SEAD).

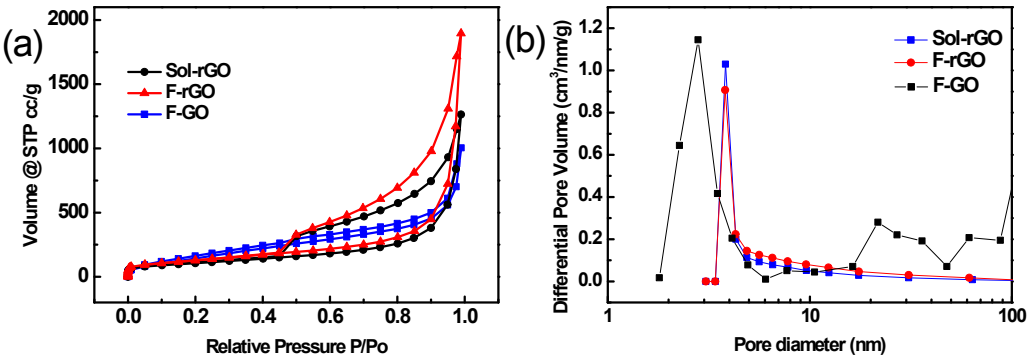

Fig. S5 N_2 adsorption-desorption isotherms and pore size distributions of Sol-rGO, F-rGO and F-GO. The N_2 adsorption-desorption isotherms of prepared products display the type IV isotherms with a distinct hysteresis loop, indicating the porous characteristics. The pore size distributions analysed by Barrett-Joyner-Halenda (BJH) method revealed that F-rGO and Sol-rGO exhibit an average pore size of 3.8 nm and F-GO shows the coexistence of hierarchical micropores and mesopores. The pore volume of Sol-rGO, F-rGO and F-GO are 3.28 cc/g, 2.24 cc/g and 2.09 cc/g, respectively.

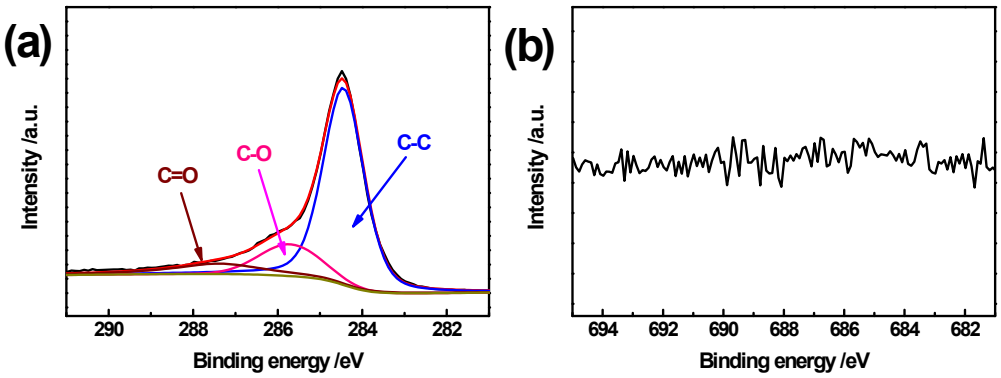

Fig. S6 a) High-resolution C1s and b) F1s spectra of Sol-rGO.

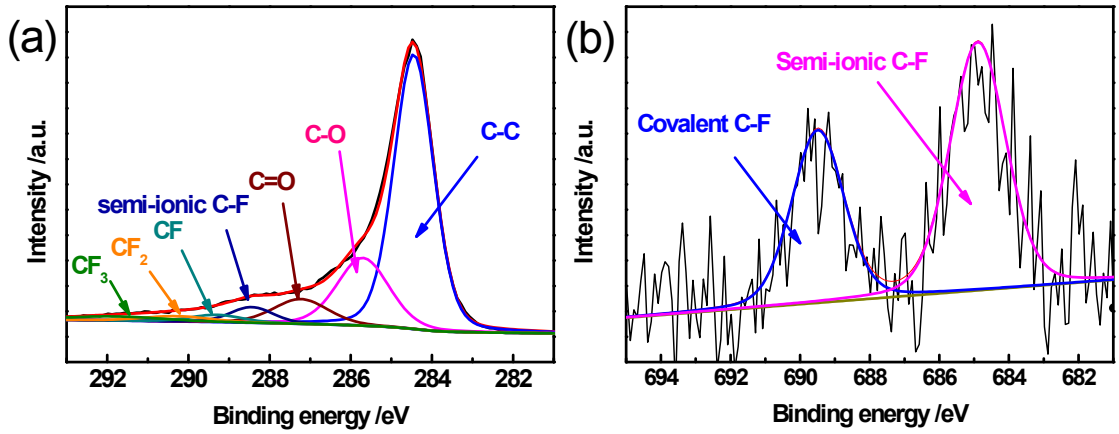

Fig. S7 a) High-resolution C1s and b) F1s spectra of F-GO. The molar ratio of semi-ionic and covalent CF, CF_2, and CF_3 groups is approximately 2.5:1:1:1, as calculated by integrating the corresponding peaks of C1s spectrum.

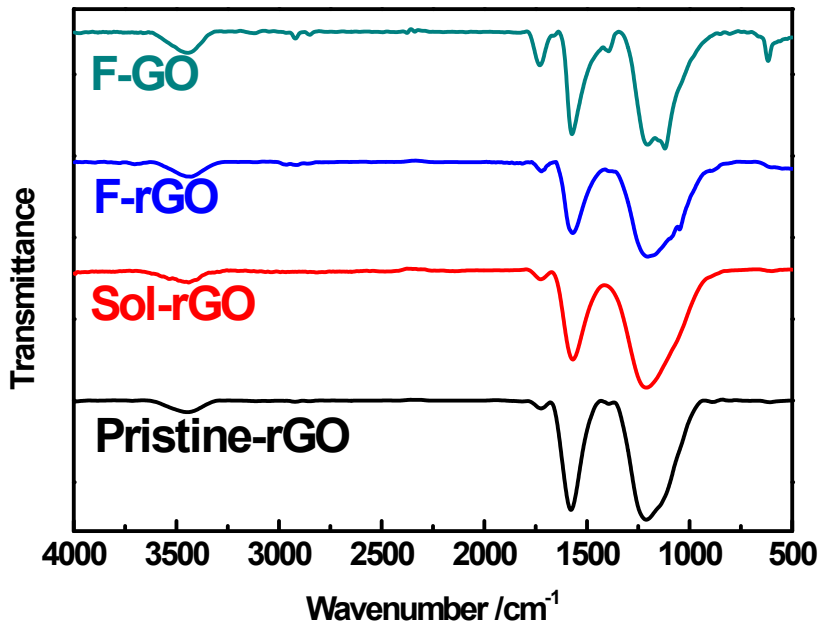

Fig. S8 FT-IR of Pristine-rGO, Sol-rGO, F-rGO and F-GO. The appearance of a peak at 1228 cm^{-1} in the spectrum is assigned to the breathing vibrational mode of the -CH(O)CH- bond, the peak at 1730 cm^{-1} is assigned to the carbonyl stretching mode of C=O and the carbonyl stretching mode of C=C at 1625 cm^{-1} are observed in the spectrum of Pristine-rGO. After fluorination and solvation, the spectrum of F-rGO and Sol-rGO seems similar, because the oxygen containing groups still exist and the overlapping of covalent C-F bonds and -CH(O)CH- bond. In the spectra of F-GO, a specific absorption peaks at 1122 cm^{-1} is observed, which is assigned to the semi-ionic C-F bonds.

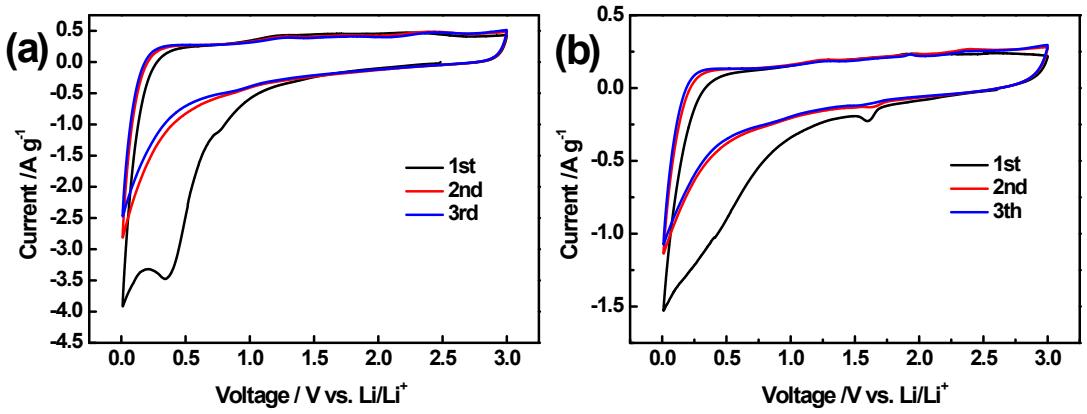

Fig. S9 CV curves of a) Sol-rGO and b) F-GO between 0.01 and 3.0 V at a potential sweep rate of 0.5 mV s^{-1}.

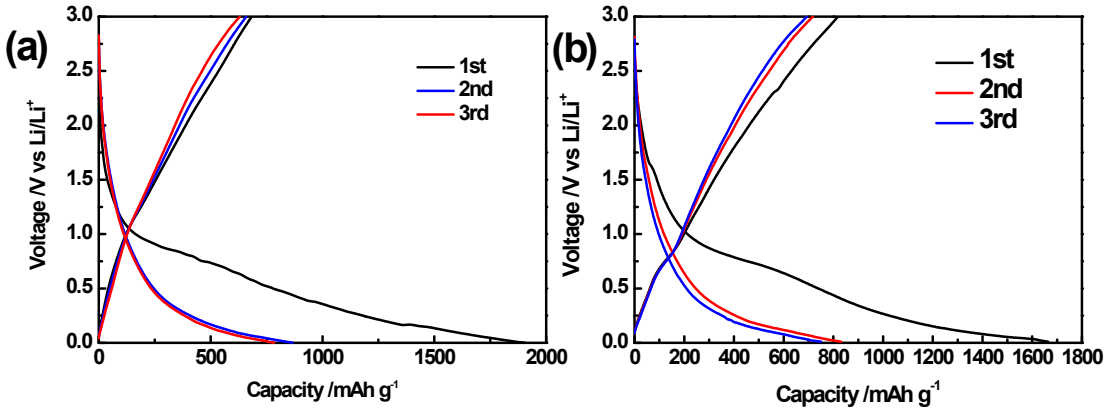

Fig. S10 Galvanostatic charge/discharge curves of the a) Sol-rGO and b) F-GO electrode at a current density of 100 mA g^{-1}.

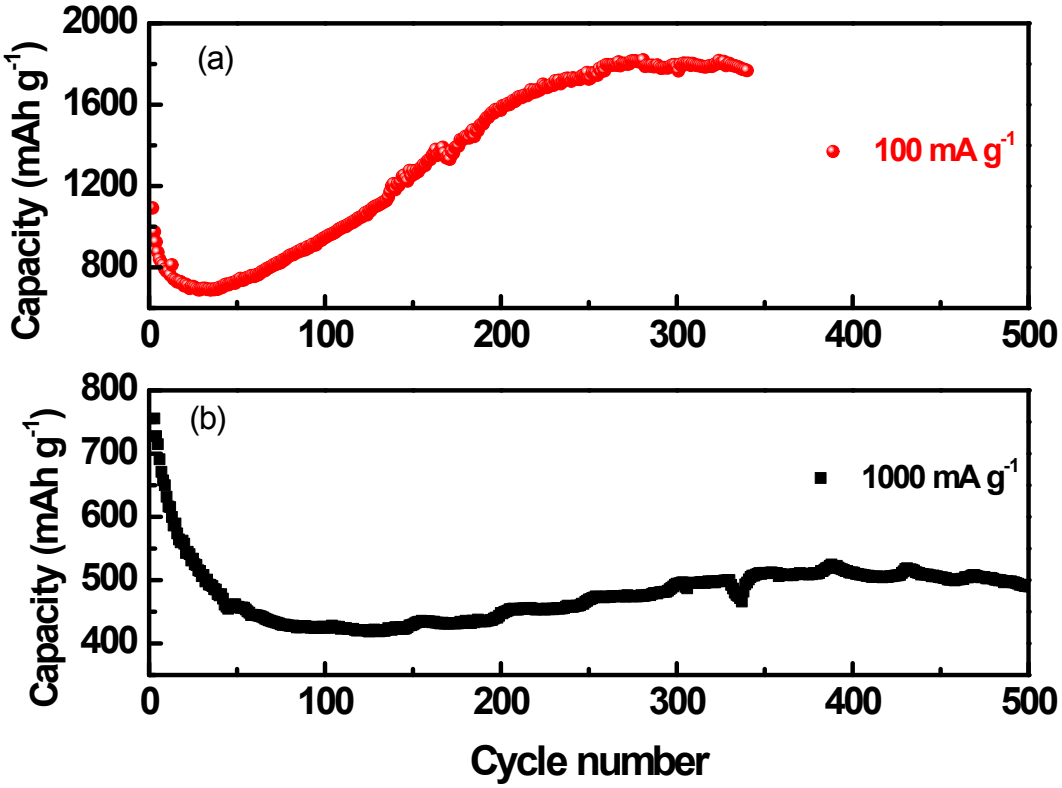

Fig. S11 Cycling performance of the F-rGO electrodes over the 0.01 to 3.0 V potential range at a current density of a) 100 mA g^{-1} a) 1000 ma g^{-1}.

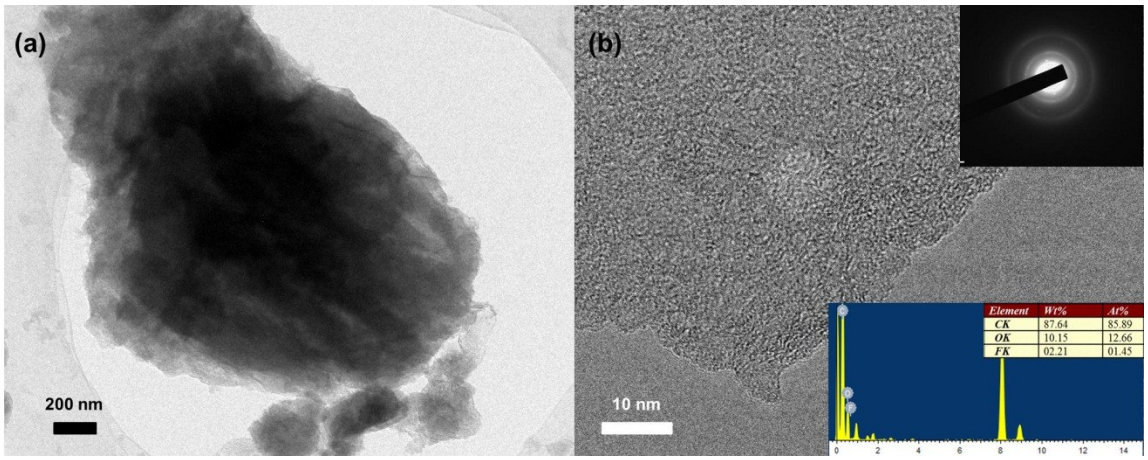

Fig. S12 a) TEM image and b) HRTEM image of F-rGO after 200 charge/discharge cycles and the the corresponding SEAD and EDX analysis.

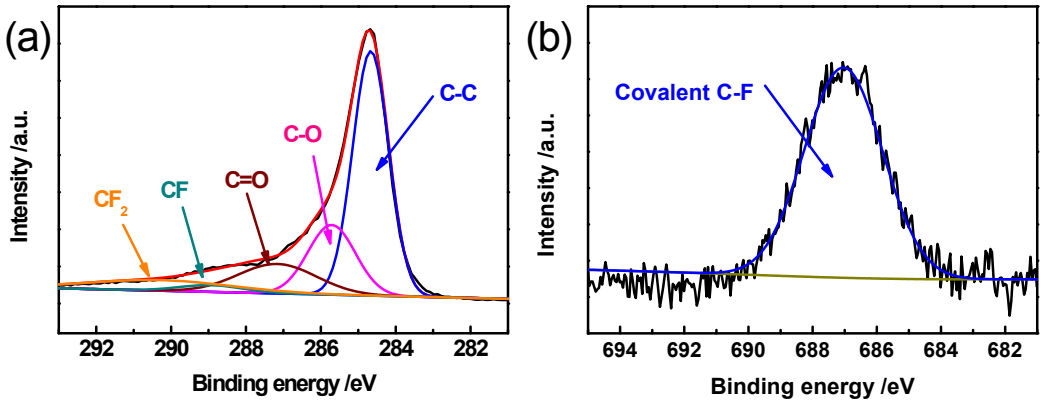

Fig. S13 a) C1s and b) F1s spectra of F-rGO after 10 charge/discharge cycles. The content of F is 2.3 At% in F-rGO and the molar ratio of CF to CF_2 groups is 1:4.

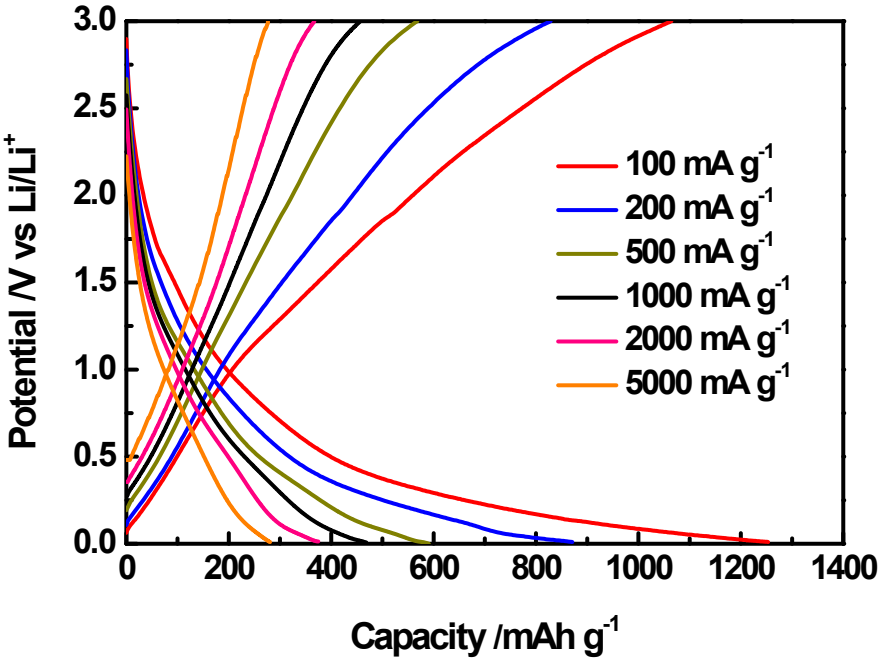

Fig. S14 The charge/discharge profiles of F-rGO electrode at current densities of 100, 200, 500, 1000, 2000 and 5000 mA g^{-1}.

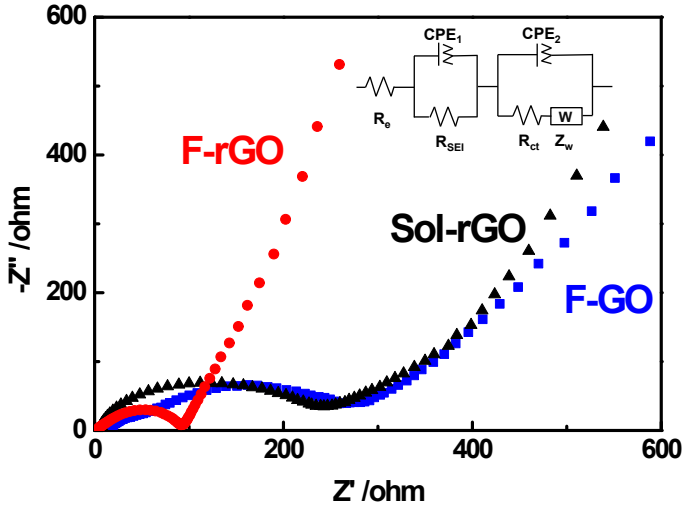

Fig. S15 Nyquist plots of F-rGO, Sol-rGO and F-GO electrodes in the charged state after 200 cycles at the current density of 100 mA g^{-1} (inset: the equivalent circuit model for simulation). The simulated values of the components according to the equivalent circuit model are listed in Table S2.

Table S1. A summary of atomic percentages of C, F, and O.

Sample	C (at.%)	O (at.%)	F (at.%)
Sol-rGO	92.0	8.0	0
F-rGO	89.3	7.3	3.4
F-GO	85.3	12.6	2.1

Table S2. Values of the equivalent circuit components used for fitting the experimental curve

Components	R_e (ohm)	CPE1-T (F)	R_{SEI} (ohm)	CPE2-T (F)	R_{ct} (ohm)
Sol-rGO	3.03	$4.31*10^{-6}$	78.29	$2.069*10^{-5}$	151.2
F-rGO	2.18	0.00139	20.45	$4.11*10^{-4}$	90.05
F-GO	8.98	$1.44*10^{-4}$	127.59	$2.72*10^{-3}$	179.56